A comparative investigation of lead-based and lead-free $MAXI_3$ perovskite solar cells with various ETLs by using SCAPS-1D

SHWETA SHUKLA, RABIN PAUL, TRUPTI RANJAN LENKA*
Department of Electronics & Communication Engineering, National Institute of Technology Silchar, Cachar, Assam, 788010, India

The photovoltaic societies are much focused and have awaited the development of the next generation of different Perovskite Solar Cells (PSCs) because of their strong prospect of supporting low-cost solar cells. This present research work emphasizes lead material $MAPbI_3$ as well as lead-free materials as $MASnI_3$ and $MAGeI_3$ perovskite solar cells using TiO_2 (Titanium dioxide) as well as ZnO (Zinc oxide) as Electron Transport Material and $CuSbS_2$ (Copper antimony sulphide) as the Hole Transport Material. It has been observed that $MAPbI_3$ gives better performance with an efficiency of 27.51% with TiO_2 as Electron Transport Layer while $MAGeI_3$ has the lowest performance of 23.25%. Furthermore, $MASnI_3$ has shown an improved result with 26.3% efficiency when ZnO is taken as Electron Transport Layer. Additionally, the performance of the various evaluated variables is almost identical to that of the perovskites under study.

(Received May 30, 2024; accepted February 3, 2025)

Keywords: $MAXI_3$, $CuSbS_2$, SCAPS-1D, Energy Conversion Efficiency, TiO_2, ZnO

1. Introduction

Researchers from all over the world are focusing more on Perovskite Solar Cells (PSCs) because of their remarkable electrical and optical properties, which include a low binding energy at an excited state, an adequate band-gap, a high coefficient of absorption, and low processing costs [1-2]. Perovskite photovoltaics demonstrated a good Energy Conversion Efficiency (ECE) of 22.86% in a short amount of time when compared to alternative methods for one-junction solar cells. As a result, they became a competitive option for the future photovoltaic market [3-4]. However, in addition to PSC instability in the ambient environment, environmental issues regarding lead-based perovskites stemming from lead's high toxicity hinder the commercialization process [5]. To create a stable, nontoxic perovskite solar cell, it is crucial to search for metal components with similar electrical properties to lead (Pb). This problem has been addressed in several articles by using Sn and Ge as an absorbent layer in place of Pb in perovskite structures. This replacement eliminates the instability caused by toxicity and moisture, but it also severely reduces the device's performance [6]. Researchers are very interested in studying the various features of this new class of perovskite material in order to improve PSC performance in addition to stability [7]. In this work, $CuSbS_2$ was utilized as the Hole Transport Layer (HTL) and TiO_2/ZnO as the Electron Transport Layer (ETL), in a comparative simulation analysis for $MAXI_3$ as absorbing material in PSC (where X=Pb, Sn, Ge). The purpose of this research is to examine how various elements affect PSC performance and, in turn, make an application of the devices based on results of the simulations. The outcomes of analysis of the PSC have been indicated by the results shown by the absorber layer thickness and defect density.

2. Methodology

2.1 SCAPS-1D and simulation framework

The one-dimensional Solar Cell Capacity Simulator (SCAPS-1D) program has been introduced in this study to simulate the performance of perovskite solar cells. Poisson's equation, carrier-continuity equation and drift-diffusion equation are the equations that control semiconductor substances for electron or hole carriers and are the foundation of the SCAPS-1D simulation approach [8-9]. Understanding the fundamentals of solar cells and identifying the key elements that influence their performance are made easier with the use of numerical modeling. The equation between an electric field (E) and space charge density (ρ) of p-n junction is represented by the Poisson equation, which is as follows [10-11].

$$\frac{\partial^2 \psi}{\partial x^2} = -\frac{\partial E}{\partial x} = -\frac{\rho}{\varepsilon_s} = -\frac{q}{\varepsilon_s}[p - n + N_D^+(x) - N_A^-(x) + N_{def}(x) \quad (1)$$

where ψ is Electrostatic potential, q is the elementary charge, p(n) is the density of hole (electron), ε_s is the relative permittivity static) of the medium and N_A (N_D) are the ionized acceptors (donors) density, and N_{def} is the defect density (acceptor or donor).

The electron hole continuity equations in equilibrium state are expressed as:

$$\frac{-\partial j_n}{\partial x} - U_n + G = \frac{\partial n}{\partial t} \quad (2)$$

$$\frac{-\partial j_p}{\partial x} - U_p + G = \frac{\partial p}{\partial t} \quad (3)$$

Here, the current density of electrons and holes are represented by j_n and j_p, the rates of net recombination by $U_{n,p}$, and the electron-hole production rate by G.

The current density of electrons as well as holes is determined by:

$$j_n = -\frac{\mu_n n}{q}\frac{\partial E_{F_n}}{\partial x} \quad (4)$$

$$j_p = +\frac{\mu_n p}{q}\frac{\partial E_{F_p}}{\partial x} \quad (5)$$

Here the elementary charge is denoted by q, the electron (or hole) mobility by $\mu_{n(p)}$, and the electron (or hole) diffusion coefficient by $D_{n(p)}$.

Numerous studies that have been published in the literature, including [12-14], attest to the fact that data from the SCAPS program closely match with actual findings. It therefore validates and makes the simulation results in this investigation trustworthy.

2.2. Device configuration and absorber layer parameters

Table 1 lists the various parameters of perovskite materials that have been gathered from the literature [1, 2,6,13-26] and Table 2 lists the FTO, ETL, and HTL characteristics. The AM1.5G spectrum (1000 Wm^{-2}) was used to illuminate the device from the ETL side during the simulation, which was conducted in direct sunlight with an assumed ambient temperature of 300 K. Figs. 1 and 2 depict the configuration of the PSC devices and energy levels of the utilized materials, respectively.

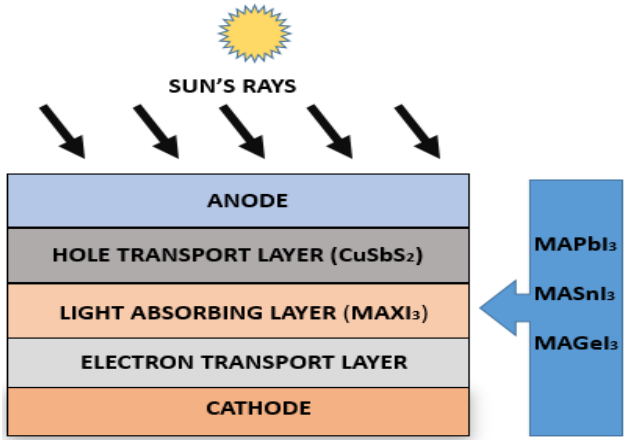

Fig. 1. Configuration of the PSC devices (color online)

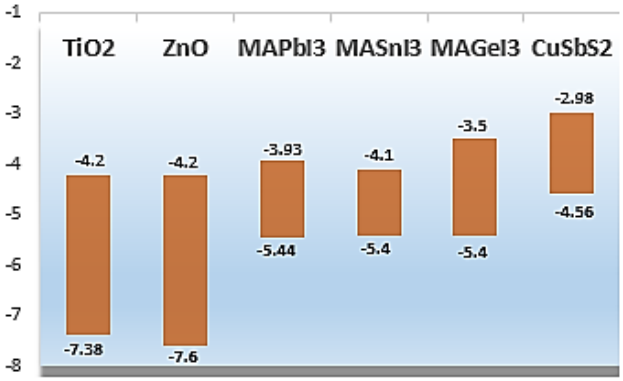

Fig. 2. Energy levels for all materials used in the study (colour online)

Table 1. Material Parameters of different $MAXI_3$ materials used in this study

Material Property	**$MAPbI_3$**	**$MASnI_3$**	**$MAGeI_3$**
Thickness (nm)	200-1400	200-1400	200-1400
Band gap (eV)	1.5	1.3	1.9
Electron Affinity (eV)	3.75	4.2	3.98
Dielectric Permittivity	6.5	10	10
Conduction Band effective Density of States (per cm^3)	1×10^{18}	1×10^{18}	1×10^{16}
Valence Band effective Density of States (per cm^3)	1×10^{18}	1×10^{18}	1×10^{15}
Mobility of Electron (cm^2/V_S)	2	1.6	2
Mobility of Hole (cm^2/V_S)	2	1.6	2
Donor Density, per cm^3	1×10^{9}	0	1×10^{9}
Acceptor Density, per cm^3	1×10^{9}	1.3×10^{18}	1×10^{9}
Defect, per cm^3	1×10^{14}	1×10^{14}	1×10^{13}
Reference	[23]	[24]	[25]

Table 2. Material Parameters of HTL, ETLs and FTO used in this study[13,26-29]

Material Property	**HTL**	**ETL(TiO_2)**	**ETL(ZnO)**	**FTO**
Thickness (nm)	80	30	50	500
Band gap (eV)	1.5	3.2	3.2	3.5
Electron Affinity (eV)	4.2	4.1	4.5	4
Dielectric Permittivity	14.6	9	10	10
Conduction Band effective Density of States (per cm^3)	2×10^{18}	1×10^{18}	1×10^{19}	1×10^{18}
Valence Band effective Density of States (per cm^3)	1×10^{19}	1×10^{19}	1×10^{19}	1×10^{19}
Mobility of Electron (cm^2/V_S)	5	20	50	20
Mobility of Hole (cm^2/V_S)	5	10	50	10
Donor Density, per cm^3	0	1×10^{18}	1×10^{15}	1×10^{19}
Acceptor Density, per cm^3	1×10^{18}	0	0	0
Defect, per cm^3	1×10^{14}	1×10^{15}	1×10^{15}	1×10^{15}

3. Results and discussion

3.1. Preliminary results

Using the SCAPS-1D, simulation study is conducted for three different types of solar cells using perovskite materials ($MAPbI_3$, $MASnI_3$, and $MAGeI_3$) as the absorber layer, $CuSbS_2$ as the Hole Transport Material, and TiO_2/ZnO as the Electron Transport Material. Table 3 presents the simulation's initial results.

The results (Table 3) indicate that the $MAPbI_3$ device is the most efficient, with an ECE of up to 27.51%. On the other hand, the $MASnI_3$ device has the largest short circuit current density (28.5 mA/cm^2), while $MAGeI_3$ has the lowest (16.47 mA/cm^2). However, in contrast to other varieties, the $MAGeI_3$ device has a greater open circuit voltage (1.73 V). By using TiO_2 material as ETL, the efficiency of $MAXI_3$ is observed to be highest except $MAGeI_3$ (Table 4).

Table 3. An overview of the preliminary findings for PSC performance parameters taken from the simulation using the device configuration with (FTO/TiO_2/Perovskite materials/$CuSbS_2$/Au)

Material	**Open Circuit Voltage (V_{OC}) (Volt)**	**Short Circuit Current Density (J_{SC}) (mA/cm^2)**	**Fill Factor (FF) (%)**	**Energy Conversion Efficiency ECE (%)**
$MAPbI_3$	1.2	26.02	88.08	27.51
$MASnI_3$	1.09	29.05	86.61	27.48
$MAGeI_3$	1.73	16.47	81.75	23.25

Table 4. An overview of the preliminary findings for PSC performance parameters taken from the simulation using the device configuration with (FTO/ZnO/Perovskite materials/$CuSbS_2$/Au)

Material	**Open Circuit Voltage (V_{OC}) (Volt)**	**Short Circuit Current Density (J_{SC}) (mA/cm^2)**	**Fill Factor (FF) (%)**	**Energy Conversion Efficiency ECE (%)**
$MAPbI_3$	1.13	26.14	81.01	23.84
$MASnI_3$	1.08	28.5	85.32	26.3
$MAGeI_3$	1.17	24.56	85.23	24.64

3.2. The effect of variation of absorber layer thickness

For each of the three $MAXI_3$ types under study, a simulation was run using the thicknesses of the absorber layer ranging from 200 nm to 1400 nm to examine the result of the thicknesses of the $MAXI_3$ absorber layer performance. For $MAPbI_3$, $MASnI_3$, and $MAGeI_3$, the optimal performance is reached at 1200 nm, 600 nm, and 1400 nm with TiO_2 as ETL whereas 600 nm, 1000 nm, and 1200 nm with ZnO as ETL, in that order. Figs. 3, 4, 5, 6, 7, and 8 display the PSCs performance parameters simulation results. The primary causes of the efficiency loss on both sides of the ideal absorber thickness are the results of charge carrier recombination and photon absorption rate. It can hold more photons by thickening the absorber layer, but at the same time, the recombination rate rises. Therefore, performance is adversely affected by any additional increase in absorber thickness over the ideal value.

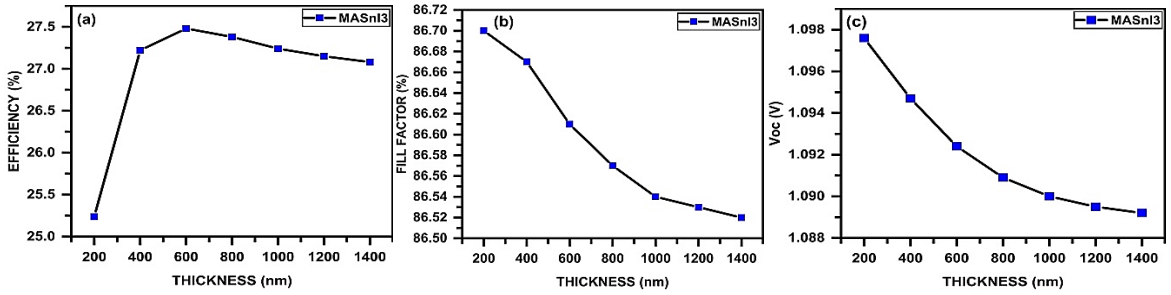

Fig. 3. Various parameters of $MASnI_3$ using TiO_2 as ETL (a) ECE (b) Fill Factor (c) V_{OC} (color online)

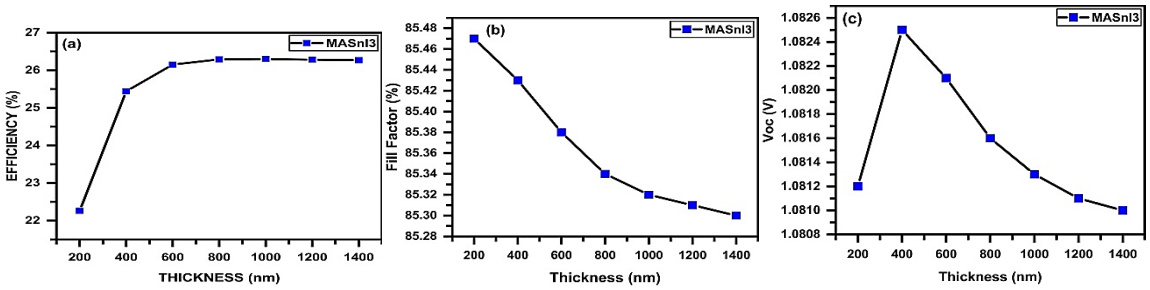

Fig. 4. Various parameters of $MASnI_3$ using ZnO as ETL (a) ECE (b) Fill Factor (c) V_{OC} (colour online)

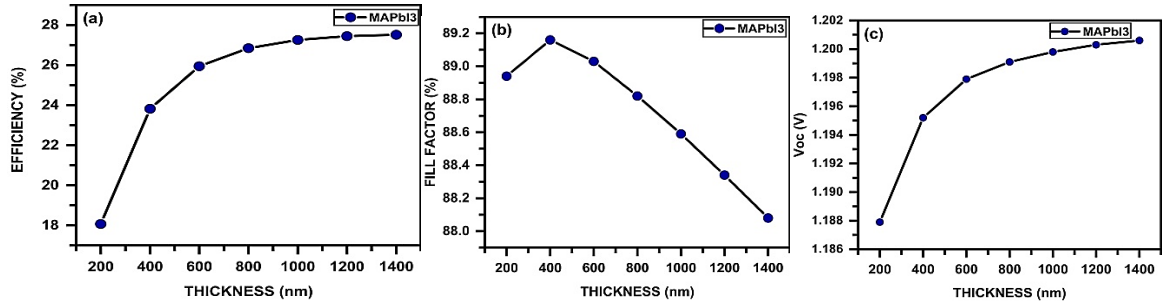

Fig. 5. Various parameters of $MAPbI_3$ using TiO_2 as ETL (a) ECE (b) Fill Factor (c) V_{OC} (colour online)

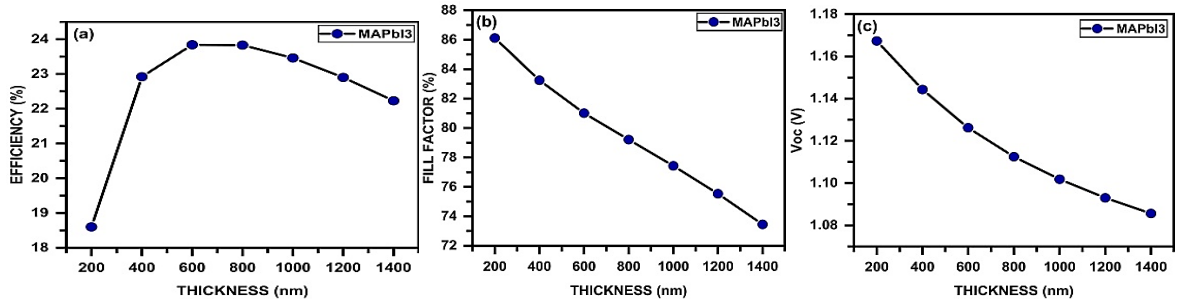

Fig. 6. Various parameters of $MAPbI_3$ using ZnO as ETL (a) ECE (b) Fill Factor (c) V_{OC} (colour online)

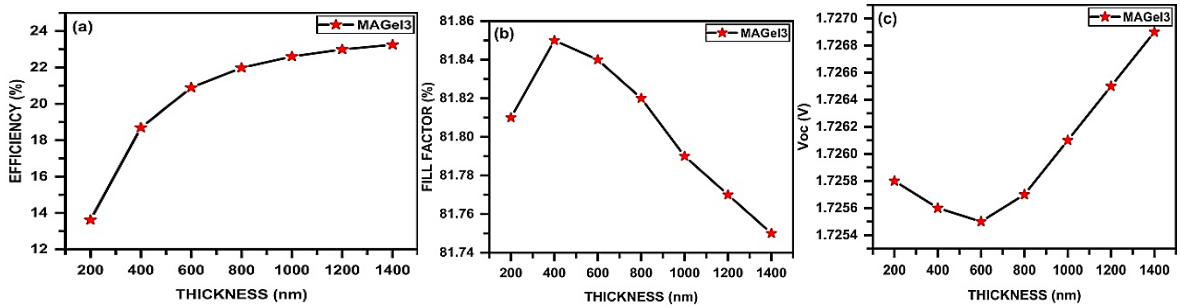

Fig. 7. Various parameters of $MAGeI_3$ using TiO_2 as ETL (a) ECE (b) Fill Factor (c) V_{OC} (colour online)

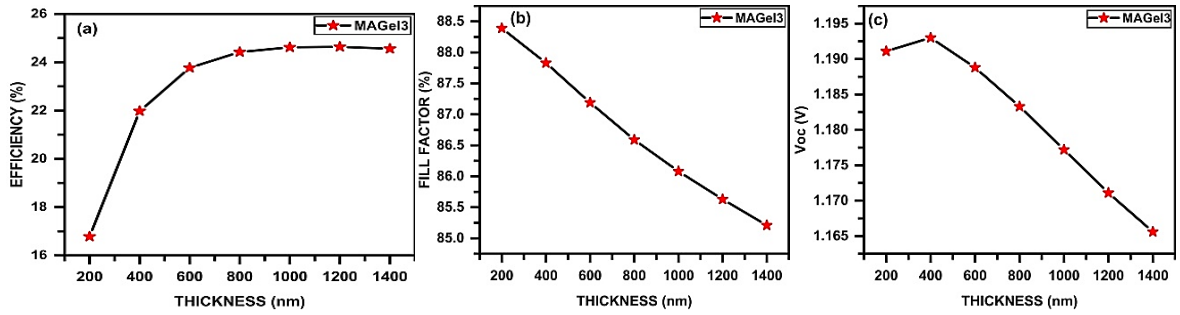

Fig. 8. Various parameters of $MAGeI_3$ using ZnO as ETL (a) ECE (b) Fill Factor (c) V_{OC} (colour online)

On the contrary, the effectiveness of PSCs is also reduced when the thickness is reduced below the ideal value for each device configuration. The reason for this is that when the active layer is too thin, fewer photons are absorbed.

Therefore, to improve PSC performance, it is crucial to find the ideal absorber thickness value that precisely balances illumination absorption and carrier transport [1].

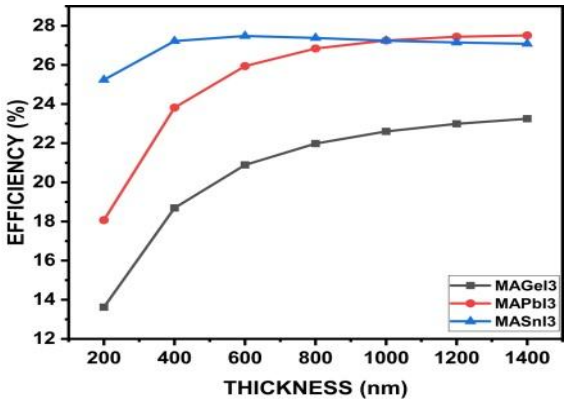

Fig. 9. Comparison study of efficiency of various PSCs using TiO_2 as ETL (colour online)

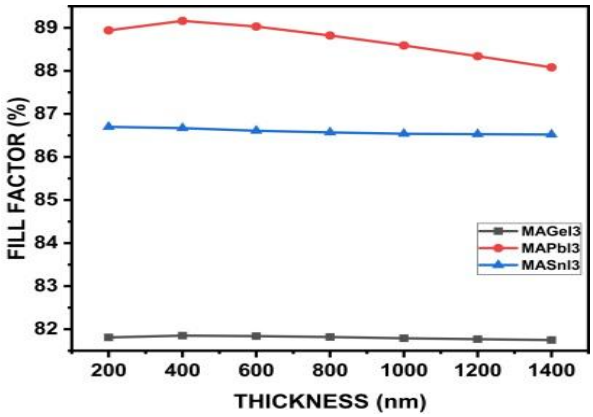

Fig. 10. Comparison study of fill factors of various PSCs using TiO_2 as ETL (colour online)

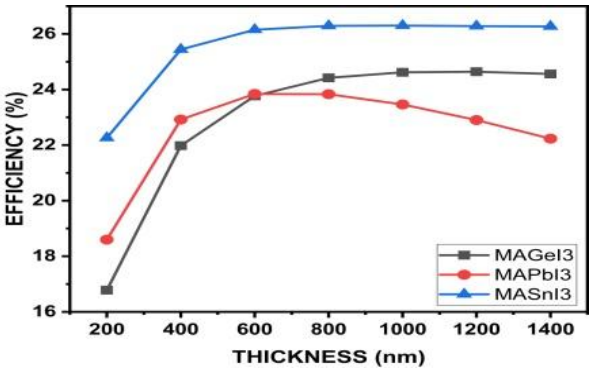

Fig. 11. Comparison study of efficiency of various PSCs using ZnO as ETL (colour online)

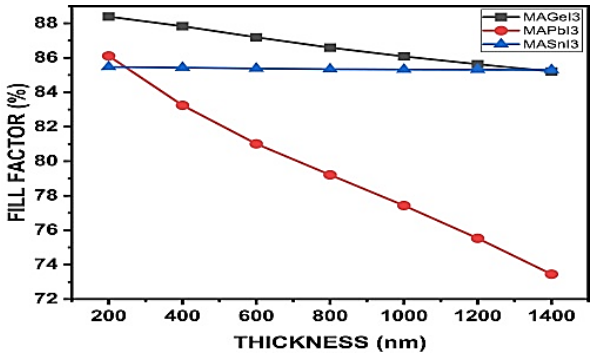

Fig. 12. Comparison study of fill factors of various PSCs using ZnO as ETL (colour online)

3.3. The ETL effect on PSCs performance

a) **Efficiency:** In the PSC, the ETL gathers electrons and obstructs the movement of holes to the FTO electrode. The ETL's mesoporous structure facilitates the crystallization and film development of perovskite while also reducing the photogenerated electrons' migratory path. While changing the electron transport material and keeping the hole transport material and various parameters the same, the performance of perovskite material is changed. With TiO_2 as HTL, the efficiency of $MAPbI_3$ is found to be maximum (27.51%) as shown in Fig. 5(a) and $MAGeI_3$ is

minimum (23.25%) given in Fig. 7(a). When ZnO is taken as ETM, the efficiency of $MASnI_3$ is found to be maximum (26.3%) as shown in Fig. 3(a).

b) **Fill Factor:** Among the most important electrical parameters used to measure the efficiency of solar cells is the fill factor (FF). A solar cell's energy conversion efficiency is correlated with its FF; a greater FF corresponds to an increased efficiency. This is indicated by comparing the results shown in Figs. 3(b), 5(b) and 7(b) that $MAPbI_3$ has maximum FF (88.08%) with TiO_2 electron transport layer and $MASnI_3$ has maximum FF (85.32%) with ZnO as ETL when checked with simulation result given in Figs. 4(b), 6(b), 8(b).

c) **Open Circuit Voltage:** It is the maximum voltage a solar cell can generate with zero current. The open-circuit voltage reflects the amount of forward bias on the solar cell caused by the bias of the solar cell junction with the light-generated current. As per comparison results, using different ETLs as shown in Figs. 3(c), 4(c), 5(c), 6(c), 7(c) & 8(c), the maximum received V_{OC}, irrespective of ETL, is of $MAGeI_3$ that is 1.73V.

Table 5 shows a comparative result of the efficiency of different perovskite cells $MAXI_3$ where X=Pb, Sn, Ge concerning recent studies. It has been observed that irrespective of ETL, material efficiency has increased up to some extent as compared with other research works.

Table 5. Comparative study of efficiency of $MAXI_3$ as obtained from literature

Material	Efficiency	Efficiency (In This Paper)	Reference
$MAPbI_3$	19.3	27.51	[30]
$MASnI_3$	22.86	27.48	[31]
$MAGeI_3$	15.84	24.64	[32]

4. Conclusion

The stability and structural features of lead-based perovskite $MAPbI_3$ play an essential role in the perovskite architecture of solar cells. However, due to lead's high toxicity, lead-free materials such as $MASnI_3$ and $MAGeI_3$ are gaining interest in the scientific community. This study explores the findings of three different absorber layers using TiO_2/ZnO and $CuSbS_2$ as Electron Transport Layer (ETL) and Hole Transport Layer (HTL) respectively. The simulation study was conducted using SCAPS-1D software on two lead-free perovskites - $MASnI_3$ and $MAGeI_3$ - as well as lead-based perovskites - $MAPbI_3$. The device is configured as FTO/TiO_2 (ZnO)/$MAXI_3$/$CuSbS_2$/Au. To optimize device configuration and increase PSC efficiency, studies have been conducted on how different factors affect the efficiency of PSC devices. These factors include the absorber layer thickness and different ETM layers. Regarding the factors under investigation, all perovskite kinds show almost the same impacts. The research, when compared with the recent findings, is found that $MASnI_3$ is giving the better result with ZnO layer whereas $MAPBI_3$ have better results with TiO_2 layer.

Acknowledgments

The authors acknowledge DST-ANRF (Anusandhan National Research Foundation), Govt. of India sponsored "Visiting Advanced Joint Research Faculty Scheme" (VAJRA) Project No. VJR/2021/000024; "Mathematical Research Impact Centric Support" (MATRICS) Project No. MTR/2021/000370, and CSIR Project No. 22(0830)/19/EMR-II) for support.

References

[1] Deepthi Jayan, Solar Energy **217**, 40 (2021).
[2] A. Raj, M. Kumar, P. K. Singh, R. Chandra Singh, H. Bherwani, A. Gupta, Materials Today: Proceedings **47**, 1564 (2021).
[3] NREL, Best Research-Cell Efficiency Chart, 2022.
[4] H. Tang, S. S. He, C. W. Peng, Nanoscale Research Letters **12**(1), 410 (2017).
[5] Patrick Tonui, Saheed O. Oseni, Gaurav Sharma, Qingfenq Yan, Renewable and Sustainable Energy Reviews **91**, 1025 (2018).
[6] M. Kumar, A. Raj, A. Kumar, A. Anshul, Optical Materials **108**, 110213 (2020).
[7] N. J. A.-T. Ehsan Raza, Zubair Ahmad, Fakhra Aziz, Muhammad Asif, Ayyaz Ahmed, Kashif Riaz, Jolly Bhadra, Solar Energy **225**, 842 (2021).
[8] S. D. M Burgelman, P Nollet, Thin Solid Films **361–362**, 527 (2021).
[9] T. R. Lenka, A. C. Soibam, K. Dey, T. Maung, F. Lin, CSI Transactions on ICT **8**(2), 111 (2020).
[10] M. Minemoto, T. Murata, Current Applied Physics **14**(11), 1428 (2014).
[11] M. Nalianya, M. A. Awino, C. Barasa, H. Odari, V. Gaitho, F. Omogo, B. Mageto, Optik **248**, 168060 (2021).
[12] H. Ş. Houimi, A. Gezgin, S. Y. Mercimek, B. Kılıç, Optical Materials **121**, 111544 (2021).
[13] S. M. B. Karimi, E. Ghorashi, Optik **130**, 650 (2017).
[14] B. J. Karthick, S. Velumani, J. Boucle, Solar Energy **205**, 349 (2020).
[15] M. Abdelaziz, S. Zekry, A. Shaker, A. Abouelatta, Optical Materials **101**, 109738 (2020).
[16] A. A. Abnavi, D. K. Maram, Optical Materials **118**, 111258 (2021).
[17] J. K. Chen, L. C. Tseng, Z. K. Huang, Nanomaterials **6**(10), 1 (2016).
[18] M. C. Gélvez-Rueda, N. Renaud, F. C. Grozema, The Journal of Physical Chemistry C **121**(42), 23392 (2017).
[19] A.-A. Kanoun M. B. Kanoun, A. E. Merad, S. Goumri-Said, Solar Energy **182**, 237 (2019).

[20] P. K. Patel, Scientific Reports **11**, 3082 (2021).
[21] N. S. Sarker, S. Islam, M. T. Rauf, A. Al Jame, S. Ahsan, M. S. Islam, M. R. Jani, S. S. Nishat, K. M. Shorowordi, S. Ahmed, Materials Today Communications **32**, 103881 (2022).
[22] A. A. Raj Abhishek, Kumar Manish, K. Singh Pramod, Singh Ram Chandra, Bherwani Hemant, Gupta Ankit, Materials Today Proceedings **47**, 1564 (2021).
[23] A. Slami, M. Bouchaour, L. Merad, International Journal of Energy and Environment **13**, 17 (2019).
[24] N. J. Valeti, K. Prakash, M. K. Singha, Results in Optics **12**, 100440 (2023).
[25] F. A. Jhuma, M. J. Rashid, S. Islam, International Exchange and Innovation Conference on Engineering and Science (IEICES), 183 (2022).
[26] N. E. Courtier, J. M. Cave, A. B. Walker, G. Richardson, J. M. Foster, Journal of Computational Electronics **18**(4), 1435 (2019).
[27] N. E. Courtier, J. M. Cave, J. M. Foster, A. B. Walker, G. Richardson, Energy and Environmental Science **12**(1), 396 (2019).
[28] Y. Raoui, H. Ez-Zahraouy, N. Tahiri, O. El Bounagui, S. Ahmad, S. Kazim, Solar Energy **193**, 948 (2019).
[29] R. Singh, A. Giri, M. Pal, K. Thiyagarajan, J. Kwak, J. J. Lee, U. Jeong, Journal of Materials Chemistry A **7**(12), 7151 (2019).
[30] C. Son, H. Son, B.-S. Jeong, Applied Sciences **14**(6), 2390 (2024).
[31] K. H. Mahmoud, A. S. Alsubaie, A. H. Anwer, M. Z. Ansari, Micromachines **14**(6), 1127 (2023).
[32] T. Al Zoubi, B. Mourched, M. Al Gharram, G. Makhadmeh, O. Abu Noqta, Nanomaterials **13**(15), 2221 (2023).

*Corresponding author: trlenka@ieee.org